Formation of a Fractal Basin Boundary in a Forced Oscillator

IAN DOBSON

Abstract—**How does a fractal basin boundary arise in the sinusoidally forced Duffing's equation? We describe how the backwards system flow deforms a local stable manifold into the fractal boundary. Parts of the boundary are labeled in a way related to their time of formation. The truncated fractal boundary produced by a burst of sinusoidal forcing is briefly considered. The approach supplements the insights provided by the usual Poincaré map techniques.**

I. Introduction

DUFFING'S equation is

$$\dot{\theta} = v$$

$$\dot{v} = \theta - \theta^3 - \delta v, \qquad (\theta, v) \in \boldsymbol{R}^2. \tag{1}$$

It has a hyperbolic equilibrium at $(0,0)$ and stable equilibria at $(\pm 1,0)$. The basin of attraction of each of the stable equilibria is defined to be the set of all initial conditions which tend to that equilibrium as time tends to infinity. The two basins are two-dimensional open sets and are separated by their common boundary, which is $W^s(0,0)$, the stable manifold of $(0,0)$ (see [1, fig. 2.2.3] or [2, fig. 1] or [3]). $W^s(0,0)$ is defined to be the set of initial conditions which tend to $(0,0)$ as time tends to infinity. The practical importance of the basin boundary $W^s(0,0)$ is that the ultimate fate of each initial condition is known once the position of $W^s(0,0)$ in phase space has been specified.

If small amplitude sinusoidal forcing is added to system 1 the equilibria become periodic orbits of small amplitude. $(0,0)$ becomes a hyperbolic periodic orbit γ and $(\pm 1,0)$ become attracting periodic orbits $\gamma_{\pm}$. $W^s(\gamma)$, the stable manifold of γ, and the basins of attraction of $\gamma_{\pm}$ are defined as the set of initial conditions tending to γ or $\gamma_{\pm}$, respectively. The basin boundary is the closure of $W^s(\gamma)$ and it separates the basin of γ_+ from the basin of γ_-. Specifying the position of $W^s(\gamma)$ determines which attractor, γ_+ or γ_-, an initial condition tends to. However, for certain parameter values, $W^s(\gamma)$ has a complicated and fractal structure [2, fig. 2]. The arbitrarily fine structure of the fractal boundary obstructs prediction of which attractor a given initial condition tends to [3].

How can a fractal boundary arise from such relatively simple, smooth equations? This question is usually answered by reducing the system to a Poincaré map whose basin boundary can be studied using embeddings of horseshoes [4], [5] or accessible saddle orbits [5], [6]. We describe the basin boundary from an alternative point of view and emphasize the temporal evolution of its fractal structure. This alternative approach should be regarded as supplementary to the usual approach; its main purpose is to provide additional insight into the fractal boundary.

For many engineering systems, forcing the equations with a constant amplitude sinusoid for all time is not realistic. For example, the forcing amplitude might be damped [7] or there may be a burst of forcing which lasts only a finite time. In the case of a burst of forcing, initial conditions eventually tend to one of the attractors for system 1 since the forcing ceases after a finite time. The basin boundary is not truly fractal, but a truncated fractal which has fractal self-similarity under several magnifications but "simple" structure at all greater magnifications. However, for practical purposes, even a truncated fractal may obstruct prediction of the ultimate fate of initial conditions. Since the truncated fractal approximates the true fractal boundary more closely as the burst time increases, one motivation for studying the case of forcing for all time is that it is the idealized limit of a system forced for a finite time.

After briefly introducing the forced Duffing's equation and sketching the usual approach to this problem, the flow in a sizeable region of phase space is linearized and part of the flow is reduced to a two-dimensional diffeomorphism on a surface of section within the linear region. The process by which this diffeomorphism deforms the local stable manifold of γ into a fractal boundary is described. A labeling scheme for parts of the boundary is presented and related to the time at which each part is formed. We suggest a way in which the theory for constant sinusoidal forcing might be applied to the case of a burst of forcing. The paper concludes by comparing the approach with the usual Poincaré map approach and indicating that the approach easily extends to attractors and the sinusoidally forced pendulum.

Manuscript received September 1, 1987. This work was supported in part by the National Science Foundation under Grant ECS8352211. This paper was recommended by F. M. A. Salam and T. Matsumoto, Guest Editors for IEEE Transactions on Circuits and Systems, July 1988.

The author is with the School of Electrical Engineering, Cornell University, Ithaca, NY 14853.

IEEE Log Number 8821327.

II. System Description

This section summarizes some basic facts about the forced Duffing's equation and mentions how the associated Poincaré map is usually studied to understand the nature of the basin boundary. A complete treatment of Duffing's equation and references to the literature may be found in [1].

When suspended in time, the sinusoidally forced Duffing's equation is

$$\begin{aligned} \dot{\theta} &= v \\ \dot{v} &= \theta - \theta^3 - \delta v + g\cos\omega t \\ \dot{t} &= 1, \qquad (\theta, v, t) \in \boldsymbol{R}^2 \times \boldsymbol{S}^1. \end{aligned} \tag{2}$$

The phase space is cylindrical with period $T = 2\pi/\omega$ in the time direction. An equivalent formulation which is also useful in this paper is to "unwrap" the circular direction of the phase space $\boldsymbol{S}^1$ so that the unwrapped phase space is $\boldsymbol{R}^2 \times \boldsymbol{R}$ and the vector field is periodic in the time direction. The plane of constant time t is denoted by Σ_t. Since $\theta - \theta^3$ is an odd function of θ, system 2 has an important symmetry. Define a map σ from the phase space to itself by $\sigma(\theta, v, t) = (-\theta, -v, t + T/2)$. Then $(\dot{\theta}, \dot{v})$ evaluated at $\sigma(\theta, v, t)$ is the negative of $(\dot{\theta}, \dot{v})$ evaluated at (θ, v, t). If the forcing amplitude g is small, system 2 has a hyperbolic periodic orbit γ near $(0,0) \times \boldsymbol{S}^1$ with Floquet multipliers λ, μ satisfying $-\mu > \lambda > 0$. γ is symmetric so that $(\theta, v, t) \in \gamma$ implies that $\sigma(\theta, v, t) \in \gamma$. The basins of attraction of the periodic orbits $\gamma_\pm$ are separated by a basin boundary which is the closure of $W^s(\gamma)$. (There may be other attractors as well.) $W^s(\gamma)$ and $W^u(\gamma)$ are immersed two-dimensional submanifolds of the phase space. Computer simulation in [2] gives evidence that simple periodic attractors and fractal basin boundaries can occur simultaneously for forcing amplitudes just above those required for transversal intersection of $W^s(\gamma)$ and $W^u(\gamma)$.

The standard way of studying the immersion of $W^s(\gamma)$ uses Poincaré maps. The Poincaré map P: $\Sigma_0 \to \Sigma_0$ is the discrete map defined by flowing along trajectories of system 2 for time T. $\gamma \cap \Sigma_0$ is a hyperbolic fixed point of P and its stable manifold (with respect to P) is identical to $W^s(\gamma) \cap \Sigma_0$. Any stable manifold may be generated by backward integrating its local stable manifold, whose position is approximately known by linear theory. Using this method to sketch $W^s(\gamma \cap \Sigma_0)$ or calculate $W^s(\gamma \cap \Sigma_0)$ by computer provides useful insight into how $W^s(\gamma)$ is immersed in phase space. If $W^s(\gamma)$ intersects $W^u(\gamma)$ away from γ the picture is complicated and the labor of drawing or calculation limits the amount of $W^s(\gamma \cap \Sigma_0)$ that can be produced. Enough of the manifold may be generated to show the features and complexity of the situation but it is hard to make sense of all of the complexity.

One approach finds a rectangular region in Σ_0 on which an iterate of P acts like Smale's horseshoe map. Then it can be shown that a cross section of $W^s(\gamma \cap \Sigma_0)$ on the rectangular region is a Cantor set and most of the cross section can be labeled using symbolic dynamics (e.g., [4]).

III. Constructing a Saddle Box

One natural way to model system 2 is to approximate it near γ by the forced linear system

$$\begin{aligned} \dot{\theta} &= v \\ \dot{v} &= \theta - \delta v + g\cos\omega t \\ \dot{t} &= 1 \end{aligned} \tag{3}$$

and then to choose a rotating coordinate system (x, y, t) which incorporates the effect of the forcing. It is also convenient to choose the x, y coordinates so as to diagonalize the system:

$$\begin{aligned} \dot{x} &= \lambda x \\ \dot{y} &= \mu y \\ \dot{t} &= 1. \end{aligned} \tag{4}$$

The linear vector field 4 is assumed in the volume $\{(x, y, t) | |x| \leqslant a, |y| \leqslant a, t \in \boldsymbol{S}^1\}$ which is referred to here as a "saddle box" of size $2a$. Outside of the saddle box the system acts to reinject into the saddle box many of the trajectories which leave the saddle box.

This view of the system as a linear flow in a saddle box with reinjection is not an approximation; it may be realized by a change of coordinates as follows. Suppose system 2 has a hyperbolic periodic orbit γ symmetric under σ with Floquet exponents λ, μ. (Note that the Floquet exponents λ, μ are close to, but not identical to the eigenvalues λ, μ obtained by diagonalising (3).) Let $\theta_m < 1/\sqrt{3}$ be the maximum θ coordinate of points on γ and let the volume $V = \{(\theta, v, t) \mid |\theta| < \theta_0\}$ where $\theta_0 < (-\theta_m + \sqrt{4 - 3\theta_m^2})/2$. (Note that θ_m is $O(g)$ so that $\theta_0 = 1 - O(g)$.) Then there is a diffeomorphic coordinate change for V under which the vector field on V is given by system 4. In particular, a saddle box may be constructed in V with respect to the new coordinates; the size of the saddle box is only limited by the saddle box not overlapping the edges of V. The coordinate change is constructed in [8]; it is based on work by Hartman on local C^1 linearization of two-dimensional diffeomorphisms without the assumption of nonresonant eigenvalues [9].

The coordinate change described above "straightens out" γ so that it becomes $(0,0) \times \boldsymbol{S}^1$ and the local stable and unstable manifolds of γ become the planes $x = 0$ and $y = 0$, respectively, inside the saddle box. The lines $l^s = \{(0, a, t) | t \in \boldsymbol{S}^1\}$ and $l^u = \{(a, 0, t) | t \in \boldsymbol{S}^1\}$ are contained in $W^s(\gamma)$ and $W^u(\gamma)$, respectively. The cylindrical nature of the phase space causes Σ_0 and Σ_T to be identified so that l^s and l^u are topological circles. The two-dimensional half sides of the saddle box are labeled as shown in Fig. 1 with their labels positioned near their respective top edges. The saddle box sides S^s and S^u are defined by $S^s = S^s_- \cup l^s \cup S^s_+$ and $S^u = S^u_+ \cup l^u \cup S^u_-$. Much of the deformation of $W^s(\gamma)$ required for $W^s(\gamma)$ to be fractally immersed in the phase space occurs as it passes near γ; linearizing the flow around γ in a saddle box allows this part of the deformation to be easily understood and calculated. One disadvantage is that the linearizing coordinate change is

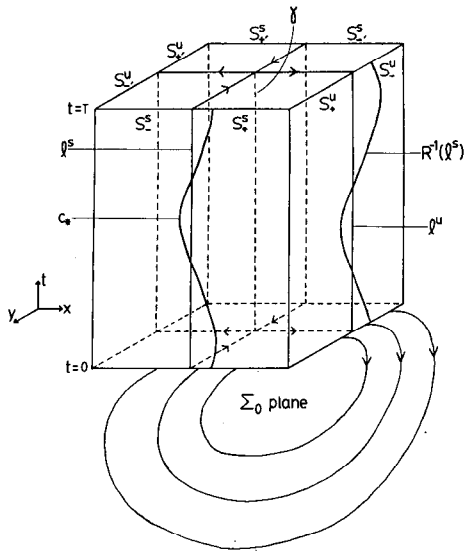

Fig. 1. Saddle box labeling. The flow outside the saddle box is suggested by the flow lines of the unforced system shown on the Σ_0 plane. The flow also has upward drift of speed unity and variation about the unforced flow due to the forcing.

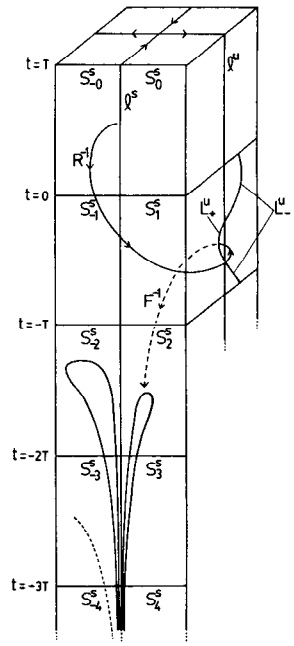

Fig. 2. First stage of fractal formation in $\boldsymbol{R}^2 \times \boldsymbol{R}$.

hard to calculate exactly and hence, for example, the exact form of the saddle box sides in the original coordinates is hard to determine. However, near γ the coordinate change is well approximated by the rotating coordinate change which transformed system 3 into system 4.

IV. Reduction of System to Discrete Maps on the Saddle Box Sides

This section shows how portions of the three-dimensional flow of system 2 may be reduced to a two-dimensional diffeomorphism on the saddle box side S^s. First note that the saddle box sides are suitable surfaces of section for the flow since the linear flow inside the saddle box is always transverse to the saddle box sides. Since the flow is also smooth, the maps induced by the flow on the saddle box sides are diffeomorphisms. R^{-1} and F^{-1} are maps on the saddle box sides induced by the backwards flow. (Here we use the convention that inverse maps correspond to the backwards flow, or integration in reverse time.) The reinjection map R^{-1} has a domain $H \subset S^s$ which is mapped into S^u according to the backwards flow outside the saddle box. (H consists of all the points in S^s which have a backward trajectory which intersects S^u on its first "opportunity" to do so.) The map F^{-1} is defined using the backwards flow inside the saddle box and exploiting the symmetry σ. The backwards flow maps points on S^u_+ to S^s_+ and points on S^u_- to S^s_-. $F^{-1}(x)$ is defined for $x \in S^u_+$ to be the first intersection with S^s_+ of the backward trajectory through x and $F^{-1}(x)$ is defined for $x \in S^u_-$ to be σ(first intersection with S^s_- of the backward trajectory through x). Thus F^{-1} maps $S^u_+ \cup S^u_-$ into S^s. F^{-1} is not defined on l^u since points on l^u tend to γ as time tends to $-\infty$ and never leave the saddle box. Any trajectory or other dynamical feature of the system which intersects S^s_-, has a counterpart under σ that intersects S^s_-. Defining F^{-1} on S^u_- using σ amounts to identifying any dynamical feature on S^s_-, with its counterpart on S^s_-.

The maps F^{-1} and R^{-1} may be combined to form a map Γ^{-1} from $H - c_*$ to S^s: $\Gamma^{-1} = F^{-1} \circ R^{-1}$. Since F^{-1} is not defined on l^u, Γ^{-1} is not defined on the curve $c_* = R(l^u)$. Appendix A sketches how Melnikov theory shows that c_* is approximately sinusoidal for small forcing and damping. Referring to Fig. 1, Γ^{-1} maps the part of H to the right of c_* to S^s_+ and the part of H to the left of c_* to S^s_-.

V. Fractal Formation

The objective is to study the immersion of $W^s(\gamma)$ in phase space by examining its intersections with the saddle box side S^s. Since $W^s(\gamma)$ is constructed by backwards integration of the local stable manifold of γ, $W^s(\gamma) \cap S^s$ may be constructed by the successive application of Γ^{-1} to l^s. Each successive application of Γ^{-1} is regarded as another stage in producing $W^s(\gamma) \cap S^s$ so that l^s is the zeroth stage and $\Gamma^{-n}(l^s)$ is the nth stage in the construction. Each application of Γ^{-1} may produce some points in S^s outside the domain of Γ^{-1} which are then effectively lost from the construction. Discussion of this difficulty is postponed to Section VII.

The main assumption causing $W^s(\gamma)$ to be fractal is that $W^s(\gamma)$ and $W^u(\gamma)$ intersect transversally somewhere other than along γ. In particular, it is assumed that c_* and l^s, or, equivalently, l^u and $R^{-1}(l^s)$ intersect transversally exactly twice. (c_* and l^s must intersect an even number of times since they are both topological circles; the approximately sinusoidal nature of c_* indicates that the number of intersections with l^s is two.) For small g and δ, Melnikov theory [1] shows that $W^s(\gamma)$ and $W^u(\gamma)$ and hence c_* and l^s intersect transversally for a suitably large ratio of g to δ. (It is easy to see this from Fig. 1, for δ controls the average

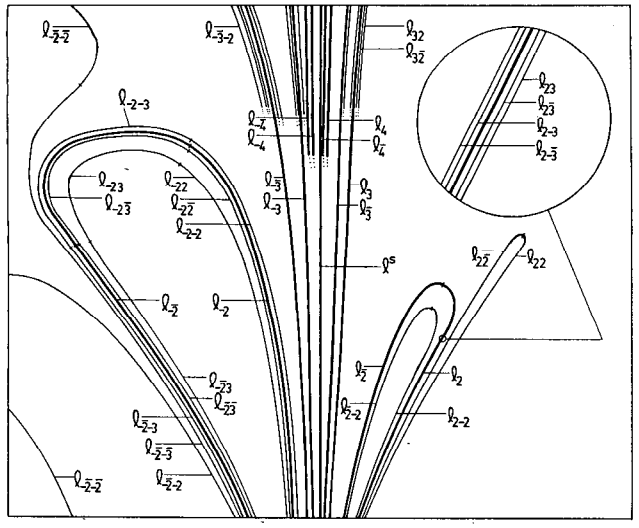

Fig. 3. First stage leaves (thick lines) and second stage leaves on S^s. Parts of the figure are distorted to show detail.

offset of c_* from l^s and g is related to the amplitude of the oscillation of c_*. If the amplitude of oscillation of c_* exceeds its average offset from l^s, it will cross l^s twice.)

The form of $\Gamma^{-1}(l^s)$ is now explained, as this is the key to understanding the fractal boundary formation. It is convenient to regard $\Gamma^{-1}(l^s)$ as being in the unwrapped phase space $\boldsymbol{R}^2 \times \boldsymbol{R}$. Since $R^{-1}(l^s)$ and l^u intersect twice, $R^{-1}(l^s) \cap S^u_+$ consists of a loop L^u_+ and $R^{-1}(l^s) \cap S^u_-$ consists of L^u_- as shown in Fig. 2. First consider how L^u_+ is mapped to its image $F^{-1}(L^u_+)$. It is easily checked by solving system 4 that the time spent inside the saddle box for backward integration of the point $(a, y, t) \in S^u$ is $\mu^{-1} \ln |y/a|$. The curved portion of L^u_+ which is not adjacent to l^u spends a moderate amount of time inside the saddle box and emerges as a distorted curve on S^s_+ at a negative time of moderate magnitude. The portion of L^u_+ close to l^u passes close to γ, spends a long time inside the saddle box and emerges greatly distorted at a negative time of large magnitude. Indeed the distortion for points (a, y, t') near l^u (i.e., small y coordinate greater than zero) may be calculated. Backward integration of system 4 yields

$$(x, a, t) = F^{-1}(a, y, t') = \left(\left| \frac{y}{a} \right|^{-\lambda/\mu}, a, t' - \mu^{-1} \ln \left| \frac{y}{a} \right| \right)$$

where t' is bounded within $[0, T)$ so that for small $y > 0$

$$t \approx -\mu^{-1} \ln \left| \frac{y}{a} \right| = \lambda^{-1} \ln x \quad \text{or} \quad x \approx e^{\lambda t}$$

which is the graph in S^s of an exponential decaying to zero as t tends to $-\infty$. Thus $F^{-1}(L^u_+)$ is a loop in S^s_+ which has two "tails" extending to $t = -\infty$ and tending towards l^s like $e^{\lambda t}$. $F^{-1}(L^u_-)$ is a similar structure in S^s_- tending towards l^s from the other side. (The lower part of L^u_- maps to the dotted line shown in Fig. 2; this is shifted upwards by T to avoid the inconvenient break in the curve.) In the cylindrical phase space $\boldsymbol{R}^2 \times \boldsymbol{S}^1$, all the copies of S^s in the unwrapped phase space are identified and $F^{-1}(L^u_+ \cup L^u_-) = F^{-1}(R^{-1}(l^s)) = \Gamma^{-1}(l^s)$ is the two

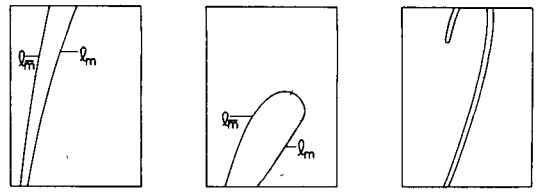

Fig. 4. Leaves in $\Gamma^{-1}(l) \cap S_m$.

loops with "chopped up" exponential tails shown as thick lines in Fig. 3. Each separately labeled portion of the curve shown in Fig. 3 is here called a "leaf." The first stage leaves and most of the leaves in succeeding stages have endpoints in Σ_0. The construction above shows how Γ^{-1} splits l^s into an infinite number of leaves which approach l^s exponentially from both sides. Thus the transversal intersection of c_* with l^s causes $W^s(\gamma)$ to accumulate on itself in the first stage of construction. In the second stage each leaf of $\Gamma^{-1}(l^s)$ close enough to l^s will also intersect c_* transversally and will similarly be split by Γ^{-1} into an infinite number of leaves accumulating on l^s. Successive applications of Γ^{-1} will produce a complicated structure of many leaves $\Lambda = \cup_{n \geq 0} \Gamma^{-n}(l^s) = W^s(\gamma) \cap S^s$. One good way to understand Λ is to try to label it systematically.

VI. Fractal Labeling

In the unwrapped phase space $\boldsymbol{R}^2 \times \boldsymbol{R}$ the part of the saddle box half-sides $S^s_\pm$ below Σ_T may be partitioned into sets $S^s_{\pm m}$ which are the time translates of $S^s_\pm \cap \boldsymbol{R}^2 \times [0, T)$ (see Fig. 2):

$$S^s_\pm \cap \boldsymbol{R}^2 \times \{t < T\} = \bigcup_{m=0}^{\infty} S^s_\pm \cap \boldsymbol{R}^2 \times [-mT, (1-m)T)$$

$$= \bigcup_{m=0}^{\infty} S^s_{\pm m}.$$

This partition may be used to label the leaves in $\Gamma^{-1}(l)$ where l is a given leaf in the cylindrical phase space $\boldsymbol{R}^2 \times \boldsymbol{S}^1$. Consider the leaves in $\Gamma^{-1}(l) \cap S^s_m$, $m \in \boldsymbol{Z}$. The leaf in Fig. 4(a) arising from the upper part of l is labeled $l_{\bar{m}}$ and the leaf arising from the lower part of l is labeled l_m. (The overbarred integers $\bar{\boldsymbol{Z}} = \{\bar{0}, \pm\bar{1}, \pm\bar{2}, \cdots\}$ are simply another distinguishable copy of the integers for labeling purposes.) If $\Gamma^{-1}(l) \cap S^s_m$ consists of a single loop as shown in Fig. 4(b) then the loop is partitioned (arbitrarily) into $l_{\bar{m}} \cup l_m$ so that $l_{\bar{m}}$ arises from the upper part of l and l_m arises from the lower part of l. Now all the leaves in $\Lambda = \cup_{n \geq 0} \Gamma^{-n}(l^s)$ may be labeled inductively with multi-indexes which are strings of elements of $Z \cup \bar{Z}$. l^s has a null index, $\Gamma^{-1}(l^s)$ is composed of leaves l_m, $\Gamma^{-1}(l_m)$ is composed of leaves l_{nm}, etc., where $m, n \in \boldsymbol{Z} \cup \bar{\boldsymbol{Z}}$ (see Fig. 3). Thus Λ is composed of leaves l_α where $\alpha = m_k m_{k-1} \cdots m_1$, $m_i \in \boldsymbol{Z} \cup \bar{\boldsymbol{Z}}$ and k is the stage at which the leaf was produced. The multi-index of a leaf encodes its formation in stages.

This labeling scheme, although helpful in organizing the leaves, is not entirely satisfactory. It can happen that $\Gamma^{-1}(l_\alpha) \cap S^s_m$ has more than two components as shown for

example in Fig. 4(c). In this case, $l_{m\alpha}$ and $l_{\bar{m}\alpha}$ refer to more than one leaf each. Also not all possible multi-indexes have leaves associated with them. For example, the first stage leaves in Figs. 2 and 3 are $\{l_2, l_3, \cdots, l_{\bar{2}}, l_{\bar{3}}, \cdots, l_{-2}, l_{-3}, \cdots, l_{-\bar{2}}, l_{-\bar{3}}, \cdots\}$; first stage leaves with indexes smaller than 2 do not exist. However, there is a large subset of leaves for which these labeling problems are avoided. Define $A_K = \{\text{multi-indexes } \alpha \mid \text{if } m \text{ is an index in } \alpha \text{ then } |m| > K\}$. Then for some suitably large K, $\Lambda_K = \{l_\alpha \mid \alpha \in A_K\}$ contains leaves which, at each stage of their formation, consist of "tails" of exponentials C^1 close to l^s. If $|m| > K$ and $\alpha \in A_K$ then $\Gamma^{-1}(l_\alpha) \cap S^s_m$ has exactly two components as shown in Fig. 4a; these are labeled $l_{m\alpha}$ and $l_{\bar{m}\alpha}$. Moreover l_α exists for each $\alpha \in A_K$. Λ_K is contained in a narrow strip around l^s; however, the narrow strip may contain leaves not in Λ_K. For example, if l_β is any leaf intersecting c_* then $l_{m\beta}$ is contained in the narrow strip for sufficiently large m.

The fractal structure arbitrarily close to l^s is reproduced around each leaf l_α of Λ. For if l_α was produced at stage n, then $\Gamma^n(l_\alpha)$ contains a segment of l^s and Γ^{-n} of a neighborhood of that segment of l^s contains l_α. Since Γ^{-n} is a diffeomorphism, the structure in that neighborhood of l^s is reproduced around l_α. For example, $l_m \to l^s$ as $|m| \to \infty$ implies that $l_{m\alpha} \to l_\alpha$ as $|m| \to \infty$. Thus each leaf of Λ is the limit of sequences of other leaves from both sides.

Λ is not the entire boundary since the boundary is a closed set and Λ is a proper subset of its closure $\bar{\Lambda}$. The Poincaré map and embedded horseshoe analysis shows that $\bar{\Lambda} - \Lambda$ is a complicated set which includes periodic orbits and their stable manifolds [1]. It is suggestive to think of $\bar{\Lambda} - \Lambda$ as being the union of leaves having multi-indexes of infinite length. Such leaves would remain arbitrarily close to Λ under iteration by Γ but are not on $W^s(\gamma)$ and never map to l^s.

VII. Fractal Generating Regions

Each stage in the construction of Λ may produce points in S^s which are lost from the subsequent stages of the construction because they lie outside $H - c_*$, the domain of Γ^{-1}. This effect may be controlled in the case of small forcing and damping by defining a fractal generating region G as explained below.

When backward integrating the local stable manifold of γ to obtain $W^s(\gamma)$, the overall effect of the system damping is that the manifold is repelled from the (forward time) attractors γ_+ and γ_- and attracted to infinity. Thus $W^s(\gamma) \cap S^s$ is formed starting with l^s and has an average tendency as it is formed to drift onto S^s_- and then to slip off the saddle box corner edge $S^s_- \cap S^u_-$. It is desirable to be able to define a region $G \subset H$ so that Γ^{-1} is defined on $G - c_*$ and in which all the fractal generation takes place. Since the only mechanism generating the fractal is the splitting by Γ^{-1} of leaves which cross c_*, G must contain c_*. Moreover, to ensure that Γ^{-1} acting on G captures all the fractal generation, G has the property that if $x \in G$ and $\Gamma^{-1}(x) \notin G$ then the backward trajectory through $\Gamma^{-1}(x)$ cannot re-enter G. This ensures that portions of leaves which are mapped outside of G by Γ^{-1} never intersect c_* under further backward integration and so are not further split. Appendix B shows how subharmonic Melnikov theory guarantees the existence of G for sufficiently small forcing and damping.

For larger values of forcing and damping Γ^{-1} may not fully capture all the fractal structure because parts of the boundary outside the domain of Γ^{-1} may be reinjected to cross c_* and further complicate the fractal structure. Thus rigorously accounting for all the fractal structure by saddle box methods seems, unfortunately, to be limited to the case of small forcing and damping. However the approach still works for larger forcing and damping if the requirement that all the fractal structure be accounted for is relaxed. Since c_* is assumed to cross l^s twice, the backward trajectories through $c_* \cap l^s$ intersect S^u on l^u. The domain of R^{-1}, H can then be chosen as some neighborhood of the intersections $c_* \cap l^s$ such as two small discs covering the respective intersections. Γ^{-1} is defined on $H - c_*$ and any leaf l_α which intersects H will have an image $\Gamma^{-1}(l_\alpha \cap H)$ for which $l_{n\alpha}$ and $l_{\bar{n}\alpha}$ intersect H for $n, \bar{n}$ larger than some sufficiently large K. Thus Γ^{-1} acting on H accounts for the subset Λ_K of the fractal structure.

VIII. Temporal Evolution of the Fractal

In applications it is important to note that the fine structure of a fractal boundary takes a long time to evolve by the process of backward integrating the local stable manifold. Indeed, the notion that the infinitely fine fractal structure takes an infinite time to evolve helps to make the occurrence of fractal basin boundaries in models of physical phenomena less strange. Thus in determining the basin boundary of system 2 by forward integrating initial conditions for some finite time, an initial condition away from the fine structure will converge near to one of the attractors while an initial condition amongst the fine structure will not converge.

The time evolution of the fractal may be quantified since the approximate evolution time of a leaf is simply related to its multi-index. It follows from the definition of the leaf labeling that $l_{m\beta}$ is formed at a time approximately mT after the formation of l_β. If l^s is considered to be formed at time zero, a leaf $l_{m_k m_{k-1} \cdots m_1}$ is formed at approximately $(m_1 + m_2 + \cdots + m_k)T$. Thus the leaves formed in time L are roughly $\{l_{m_k m_{k-1} \cdots m_1} | m_1 + m_2 + \cdots + m_k < LT^{-1}\}$.

The following paragraph speculates how the saddle box theory presented above might be applied to the case of a burst of constant amplitude forcing of finite duration. The scaling of the precision needed to determine the basin boundary is roughly estimated.

The system is assumed to have three regimes; no forcing for negative time, a burst of constant amplitude sinusoidal forcing from time 0 to time L, and no forcing after time L. The forced regime assumptions are the same as those for the previous sections. The system is considered to be a

flow suspended in time even when it is unforced. Since the system is unforced after time L, it has exactly two attractors at $(\pm 1,0)\times\{t > L\}$, each with its own basin of attraction. The basin boundary is the stable manifold of the hyperbolic orbit $(0,0)\times\{t > L\}$. The objective is to estimate the fineness of the basin boundary at time 0 (i.e., the basin boundary $\cap\, \Sigma_0$). The basin boundary at time greater than L is just $W^s(0,0)$ for the unforced system and it intersects the saddle box side S^s_- as a series of straight lines parallel to and including l^s in the saddle box coordinates appropriate to the unforced system. The basin boundary at time 0 is the basin boundary at time L integrated backwards for time L through the forced regime. If the coordinates are changed to the saddle box coordinates for the forced regime, the boundary at time L becomes a series of roughly sinusoidal curves on S^s. The construction of the boundary proceeds just as in the previous analysis except that the initial curve is not l^s, but the series of curves. However, if $W^s(\gamma)$ for system 2 is assumed to be an attractor for the backward flow in the forced regime then any curve close to l^s will asymptotically tend to $W^s(\gamma)$ for system 2. Thus the fineness of the boundary at time 0 may be estimated by the fineness of the boundary produced by backwards integrating l^s for time L. The leaves produced are estimated to be $\{l_{m_k m_{k-1}\cdots m_1} | m_1 + m_2 + \cdots + m_k < LT^{-1}\}$. Both the boundary at time 0 and its approximation for the purpose of estimating fineness are truncated fractals. The finest leaf structure arises from the indices with the highest absolute value of m, so that the leaves representative of the finest structure are $l_{\pm m}$ and $l_{\pm \bar{m}}$ where $m \approx LT^{-1}$. For large L, l_m is part of an exponential tail $\{(e^{\lambda t}, t) | -m \leqslant t + r \leqslant 1 - m\}$ (Here r is the reinjection time, t is the time inside the saddle box and $t + r$ is the total time of formation of l_m from l^s.) The x coordinate of l_m is approximately $e^{\lambda(-|m|-r)} \approx e^{-\lambda LT^{-1}} e^{-\lambda r}$. Thus the finest structure of the truncated fractal consists of exponential segments such as l_m whose x coordinates scale like $e^{-\lambda LT^{-1}}$. Therefore the minimum distance between $l_{\pm m}$, $l_{\pm \bar{m}}$ and l^s and hence the measurement precision required to distinguish all parts of the boundary scale like $e^{-\lambda LT^{-1}}$. If the measurement precision or system noise length scale exceeds the minimum distance, then deterministic prediction at time 0 of which attractor the system will tend to must fail in at least part of the phase space.

IX. Conclusions

Insight into the fractal immersion of $W^s(\gamma)$ may be gained by studying its intersection with the saddle box sides as it evolves from the local stable manifold. Fractal formation requires the transversal intersection of $W^s(\gamma)$ and $W^u(\gamma)$ and occurs for a sufficiently large forcing amplitude to damping ratio (this conclusion is well known). The distortion of surfaces required to form the fractal may be understood by considering the effect of a backwards linear flow in a saddle box on curves on the saddle box side S^u. For small forcing and damping the two-dimensional map Γ^{-1} completely captures the fractal formation. It is clear that fractal formation occurs at higher values of forcing and damping, but not all the features of the boundary are accounted for by Γ^{-1}. Parts of $W^s(\gamma)$ intersecting the saddle box side S^s may be labeled to indicate how they were formed from the local stable manifold and their approximate time of formation. The importance in applications of considering when the various parts of the boundary are formed is emphasized.

This paper only considers the basin boundary of the forced Duffing's equation. However the saddle box method applies with equal force to other important examples. The method applies to the sinusoidally forced, damped pendulum for small forcing and damping. (The suspended phase space is $S^1 \times R \times S^1$ and the reinjection to the saddle box occurs via the periodicity in the pendulum angle.) By integrating the local unstable manifold forward in time to study the intersection of $W^u(\gamma)$ with S^u, the (presumed) strange attractor $\overline{W^u(\gamma)}$ of the forced Duffing's equation and the forced pendulum can also be studied using the saddle box method.

The Poincaré map and saddle box approaches are similar but are suggestive of different insights. They are similar in that the Poincaré map is a diffeomorphism on Σ_0 whereas Γ^{-1} is a diffeomorphism on the saddle box side S^s. Indeed, the system flow maps $W^s(\gamma)\cap S^s$ into $W^s(\gamma) \cap \Sigma_0$. More work is required to define Γ^{-1} than the Poincaré map. The saddle box approach exploits the system symmetry σ to simplify the formation of $W^s(\gamma)$. The two approaches treat time differently. The Poincaré map advances time by the system period T every iteration while each iteration of Γ^{-1} corresponds to decreasing time by an amount which varies to infinity. It is natural in the saddle box approach to partition $W^s(\gamma)\cap S^s$ with Σ_0 and label the leaves accordingly; this differs from the natural partitions of $W^s(\gamma)$ in the Poincaré map approach. Thus the saddle box approach encourages new ways of labeling and organizing parts of the basin boundary. In future work, the author hopes to use the leaves on the saddle box side to reduce the generation of the basin boundary to a one-dimensional map in a natural way.

Appendix A
c_* is Approximately Sinusoidal

Choose a point q on the homoclinic orbit of the unforced, undamped system so that the plane Q normal to the vector field at q is close to the saddle box side S^s of the forced and damped system. When small forcing and damping of order ϵ are turned on, Melnikov theory [1] shows that $W^u(\gamma)\cap Q$ is a sinusoidal curve to order ϵ. "Projecting" $W^u(\gamma)\cap Q$ onto S^s along the system flow to obtain $c_* = W^u(\gamma)\cap S^s$ will not alter its sinusoidal character since S^s is close to Q. Changing coordinates according to Section III in order to "straighten out" S^s will also preserve the sinusoidal character of c_* since the coordinate change is approximately the rotating coordinate change transforming system 3 into system 4.

APPENDIX B
APPLICATION OF SUBHARMONIC MELNIKOV THEORY

First consider the unforced, undamped system; this has a periodic orbit η of period $(m+(1/2))T$ inside the homoclinic loop which contains the saddle box corner edge $S^s_+ \cap S^u_+$ for some integer m. (The saddle box supplied by the theorem in [8] is large enough to allow a small value of m to be chosen.) When positive forcing and damping of order ϵ are turned on, η is no longer a periodic orbit (only orbits of period mT are preserved) and subharmonic Melnikov theory [1] shows that for small enough ϵ, $P^{2m+1}(\eta)$ lies inside η to order ϵ. Integrating η forward for a time $(2m+1)T$ forms a cylinder in $\boldsymbol{R}^2 \times \boldsymbol{R}$ whose intersection with any time slice Σ_t is close to η. The volume V inside this cylinder and all its $(2m+1)T$ time translates in $\boldsymbol{R}^2 \times \boldsymbol{R}$ is then an invariant volume only intersecting the saddle box in S^s_+ and S^u_+ and containing $S^s_+ \cap S^u_+$. By similarly applying subharmonic Melnikov theory to an orbit $\hat{\eta}$ outside the homoclinic loop of period $2\hat{m}$ (only odd subharmonics are preserved outside the homoclinic loop), we obtain a volume $\hat{V}$ which is backward invariant under the flow and which intersects the saddle box only in the sides S^s_-, S^u_-, S^s_-, S^u_- and contains the saddle box corner edges $S^s_- \cap S^u_-$, and $S^s_- \cap S^u_-$. Backward trajectories starting in $G' = S^s - ((V \cup \hat{V}) \cap S^s)$ cannot enter V since V is invariant and, if they enter $\hat{V}$, cannot leave $\hat{V}$ since $\hat{V}$ is backward invariant. Define G to be $G' \cap H$. Suppose $x \in G$ and $\Gamma^{-1}(x) \notin G$. If $\Gamma^{-1}(x) \notin G'$ then $\Gamma^{-1}(x) \in \hat{V}$. If $\Gamma^{-1}(x) \notin H$ then the backward trajectory through $\Gamma^{-1}(x)$ does not intersect S^u and so must intersect $\hat{V}$ because of the way in which $\hat{V}$ encloses the saddle box corner edges. In either case the backward trajectory through $\Gamma^{-1}(x)$ remains in $\hat{V}$ and cannot re-enter G.

ACKNOWLEDGMENT

The author thanks D. F. Delchamps, M. Varghese, and J. S. Thorp for discussion and encouragement.

REFERENCES

[1] J. Guckenheimer and P. Holmes, Nonlinear Oscillations, Dynamical Systems, and Bifurcations of Vector Fields. New York, Springer-Verlag, 1983.
[2] F. C. Moon and G-X. Li, "Fractal basin boundaries and homoclinic orbits for periodic motion in a two well potential," *Phys. Rev. Lett.*, vol. 55, no. 14, pp. 1439–1442, Sept. 1985.
[3] S. W. McDonald, G. Grebogi, E. Ott, and J. A. Yorke, "Final state sensitivity: an obstruction to predictability," *Phys. Lett. A*, vol. 99, no. 9, pp. 415–418, 1983.
[4] K. Hockett and P. Holmes, "Josephson's junction, annulus maps, Birkhoff attractors, horseshoes and rotation sets," Ergod. Theory Dyn. Syst., vol. 6, pp. 205–239, 1986.
[5] K. T. Alligood, L. Tedeschini-Lalli, and J. A. Yorke, "Metamorphoses: Sudden jumps in basin boundaries," preprint, George Mason Univ., Fairfax, VA, Dec. 1985.
[6] C. Grebogi, E. Ott, and J. A. Yorke, "Basin boundaries metamorphoses: changes in accessible boundary orbits," *Physica 24D*, pp. 243–262, Jan./Feb. 1987.
[7] M. Varghese and J. S. Thorp, "Truncated fractal basin boundaries in forced pendulum systems," *Phys. Rev. Lett.*, vol. 60, no. 8, pp. 665–668, Feb. 1988.
[8] I. Dobson, "Describing complicated basin boundaries in a forced oscillator," chap. 3, Ph. D. dissertation, Cornell Univ., Ithaca, NY, 1989.
[9] P. Hartman, "On local homeomorphisms of Euclidean space," *Soc. Matematica Mexicana Boletin*, vol. 5, pp. 220–241, Oct. 1960.

✠

Ian Dobson received the B.A. degree in mathematics from Cambridge University, Cambridge, U.K., in 1978. At present he is working toward the Ph.D. degree in electrical engineering at Cornell University, Ithaca, NY.

From 1978 to 1983 he worked for EASAMS Ltd., Surrey, England, including simulation of power supplies on contract to Culham Laboratory (United Kingdom Atomic Energy Authority). His interests include simulation of switching circuits, nonlinear dynamics, and voltage collapse in power systems.